Application of subspace identification on the recorded seismic response data of Pacoima Dam

I-No Yu[1a], Shieh-Kung Huang[1,2b], Kenneth J. Loh[3c] and Chin-Hsiung Loh[*1,3]

[1]*Department of Civil Engineering, National Taiwan University, Taipei 10617, Taiwan*
[2]*National Center for Research on Earthquake Engineering, NARLabs, Taipei, Taiwan*
[3]*Department of Structural Engineering, University of California-San Diego, La Jolla, CA 92093, USA*

Abstract.   Two seismic response data from the CSMIP strong motion instrumentation of Pacoima dam are selected: San Fernando earthquake (Jan 13, 2001; ML=4.3) and Newhall earthquake (Sept. 1, 2011; ML=4.2), for the identification of the dam system. To consider the spatially nonuniform input ground motion along the dam abutment, the subspace identification technique with multiple-input and multiple-output is used to extract the dynamic behavior of the dam-reservoir interaction system. It is observed that the dam-reservoir interaction is significant from the identification of San Fernando earthquake data. The influence of added mass (from the reservoir) during strong ground motion will create a tuned-mass damper phenomenon on the dam body. The fundamental frequency of the dam will be tuned to two different frequencies but with the same mode shapes. As for the small earthquake event, the dam-reservoir interaction is insignificant.

Keywords: subspace identification; stabilization diagram; dam-reservoir interaction

1. Introduction

In recent years, system identification techniques have been widely applied to estimate the dynamic properties of building structures. For example, system identification of high-rise buildings using shear-bending model and ARX model (Fujita *et al*. 2015). Very few papers discussed the dynamic properties of dam during earthquake excitation from the viewpoint of system identification. The major reason is lack of earthquake observation data collected from dam, besides, less strong motion instrumentation on the current existence of the dam. Due to the complicated dynamic behavior of the large civil infrastructure (dam), particularly the interaction between dam and water, system identification on the seismic response of dam becomes a very challenge one. One of the well-instrumented strong motion arrays on dam is the Fei-Tsui arch dam (Taiwan). Some seismic response data were collected from this dam since 1989. In order to consider the nonuniform excitation of the dam and detect the global dynamic behavior of the dam


∗Corresponding author, Adjunct Professor (UCSD), E-mail: lohc0220@ntu.edu.tw
[a] Student, E-mail: r05521229@g.ntu.edu.tw
[b] Ph.D., Research Associate, E-mail: sghuang@ncree.narl.org.tw
[c] Ph.D., Professor, E-mail: kenloh@ucsd.edu

(a)

(b)
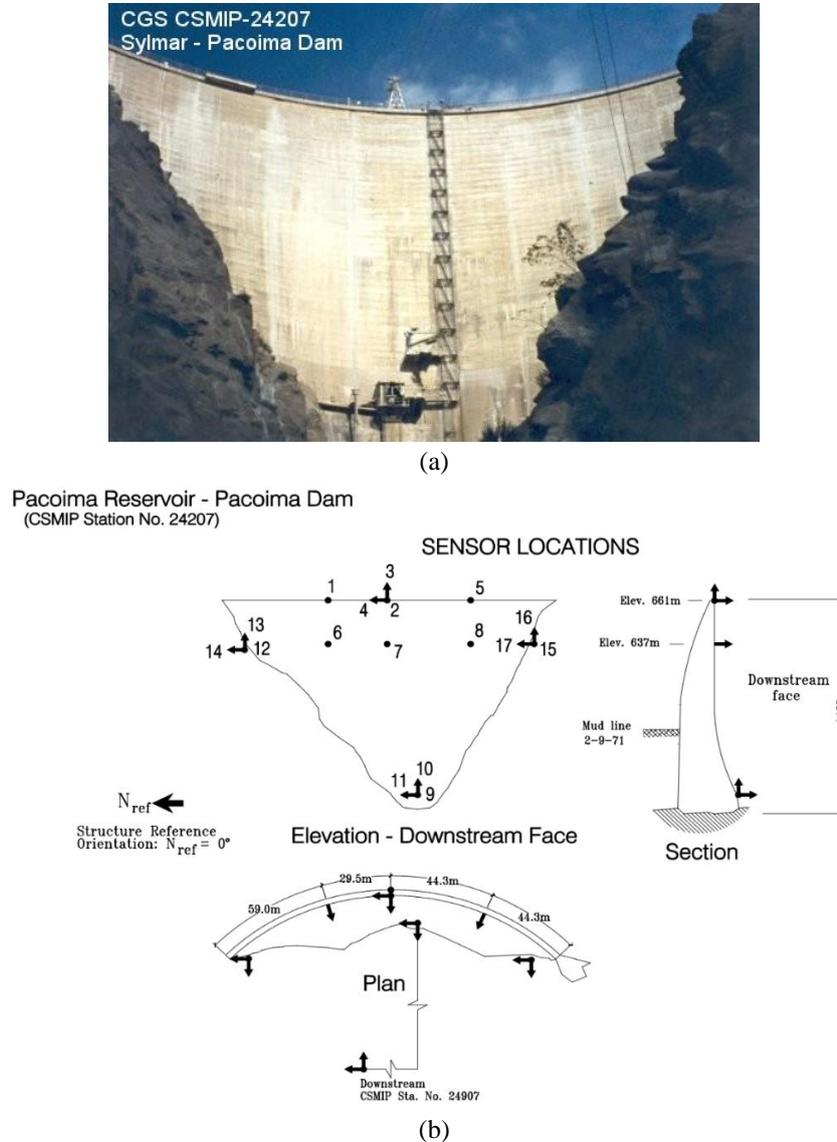
Fig. 1 (a) Photo of the Pacoima dam and (b) Distribution of seismometers on the Pacoima dam

body, multiple input ground motion along the boundary of the dam needs to be considered. Therefore, to consider this nonuniform input ground motion, the multiple-input discrete-time ARX model with least square estimation was used for the identification of the dam (Loh *et al.* 2000). The other well-instrumented arch dam is the Pacoima dam. Pacoima Dam is a 113 m high concrete arch dam located north of the city of Los Angeles. The length of the dam crest is 177.1 m. Since 1977 a total of 24 recording channels was deployed on Pacoima Dam, installed by CSMIP, as shown in Fig. 1. There were several earthquake event data had been recorded by this earthquake monitoring system, including 2001-San Fernando earthquake, 1994-Northridge earthquake, and 1987-Whittier earthquake, etc.

Many offline system identification algorithms that can be implemented for time-invariant system with constant modal parameters were developed in the past, such as the Kalman filter technique, Eigensystem realization algorithm (ERA) (Juang 1994) and auto-regressive with exogenous input model (ARX model) (Ljung 1994, Söderström *et al.* 1989), to extract the dynamic characteristics of the structural system. Most recently, the offline subspace identification technique has successfully applied on structural system identification. Good recent overview papers of the whole class of SI algorithms can be found (Rao *et al*. 1992, Van Der Veen *et al.* 1993, Viberg *et al*. 1994, Van Overschee 1996). Besides, reviews on innovations and applications in structural health monitoring for infrastructures also has been conducted (Li *et al*. 2014). Several well-known offline SI algorithms, including canonical variable analysis (CVA), numerical algorithms for subspace state space system identification (N4SID), multivariable output-error state space algorithm (MOESP), and Instrumental Variable-subspace state space system identification (IV-4SID) (Larimore 1994, Van Overschee *et al*. 1994, Verhaegen 1994), have been developed. An important achievement of the research in the subspace identification is to demonstrate how the Kalman filter states can be obtained from input/output data by using the numerical tools (singular value decomposition and QR decomposition) (Van Overschee 1996). A comparison between subspace identification and prediction error methods is made on the basis of computational complexity and precision of the methods was also discussed (Favoreel *et al.* 2000). Extension of the subspace identification to recursive subspace identification of time-varying linear systems was also developed (Kameyama *et al.* 2005, Oku 2007).

In this study, two seismic records (San Fernando earthquake and Newhall earthquake) collected from the Pacoima dam are used to identify the dynamic characteristics of the dam. Subspace identification techniques with multiple inputs (considering the spatially nonuniform ground excitation along the abutment of the dam) and multiple outputs (responses from the dam body) is used to identify the model frequencies and mode shapes of the dam. Discussion of the differences from the system identification of the dam between these two seismic events is made. Influence of dam-water interaction on the result of identification is examined between these two-event data.

2. Subspace identification algorithm

Subspace identification is a method used in identifying system matrices of the state space directly from the input/output measurements by an efficient numerical algorithm. It has been successfully tested on the structural system during past years. The structural dynamic properties can be identified from the state space linear model and directly obtained from the input and output data.

2.1 Basic theory of subspace identification

Consider the discrete-time state space model as following

$$\boldsymbol{X}(t+1) = \boldsymbol{A_d} \cdot \boldsymbol{X}(t) + \boldsymbol{B_d} \cdot \boldsymbol{u}(t) + \boldsymbol{w}(t)$$

$$\boldsymbol{y}(t) = \boldsymbol{C_c} \cdot \boldsymbol{X}(t) + \boldsymbol{D_c} \cdot \boldsymbol{u}(t) + \boldsymbol{v}(t) \tag{1}$$

where $\mathbf{u}(t)$ is inputs, $\mathbf{y}(t)$ is outputs, $\mathbf{X}(t)$ is a state vector, $\mathbf{w}(t)$ is a process noise sequence and $\mathbf{v}(t)$ is the measurement disturbances. Assume that the system is stable and observable, the original

state space model can be transformed into the "Matrix Input-Output Equations" for system identification and expressed in the following equations (Van Overschee 1996)

$$Y_p = \Gamma_i \cdot X_p + H_i \cdot U_p + G_i \cdot W_p + V_p$$

$$Y_f = \Gamma_i \cdot X_f + H_i \cdot U_f + G_i \cdot W_f + V_f \tag{2}$$

$$X_f = A_d^{\ i} \cdot X_p + \Delta_i \cdot U_p$$

with

$$\Gamma_i \equiv \begin{bmatrix} C_c \\ C_c A_d \\ C_c A_d^{\ 2} \\ \vdots \\ C_c A_d^{\ i-1} \end{bmatrix} \in \mathrm{R}^{li \times 2n} \qquad H_i \equiv \begin{bmatrix} D & 0 & 0 & \cdots & 0 \\ C_c B_d & D & 0 & \cdots & 0 \\ C_c A_d B_d & C_c B_d & D & \cdots & 0 \\ \vdots & \vdots & \vdots & \ddots & \vdots \\ C_c A_d^{\ i-2} B_d & C_c A_d^{\ i-3} B_d & C_c A_d^{\ i-4} B_d & \cdots & D \end{bmatrix} \in \mathrm{R}^{li \times mi}$$

$$G_i \equiv \begin{bmatrix} 0 & 0 & 0 & \cdots & 0 \\ C_c & 0 & 0 & \cdots & 0 \\ C_c A_d & C_c & 0 & \cdots & 0 \\ \vdots & \vdots & \vdots & \ddots & \vdots \\ C_c A_d^{\ i-2} & C_c A_d^{\ i-3} & C_c A_d^{\ i-4} & \cdots & 0 \end{bmatrix} \in \mathrm{R}^{li \times 2ni}$$

and

$$\Delta_i \equiv \begin{bmatrix} A_d^{\ i-1} B_d & A_d^{\ i-2} B_d & \cdots & A_d B_d & B_d \end{bmatrix} \in \mathrm{R}^{2n \times mi}$$

where Γ_i is extended observability matrix which contains information of system matrices (i.e., A_d and C_d), and it is the primary outcome of the subspace identification. From the matrix input-output equations (Eq. (2)), the future input Hankel matrix, U_f, can be eliminated by projecting the whole equation onto the orthogonal component of the future input matrix. Since the process errors as well as the measurement errors are assumed to be independent of "the instrumental variables (IV), Ξ_p", which is assigned to be composed of past input, U_p, and past output, Y_p, data matrix, the projected equation is multiplied by the transpose of IV matrix. Then, the resultant projection matrix, $O_{(k)}^{orthogonal}$, derived from the above-mentioned procedure contains the information of the target extended observability matrix, Γ_i.

It is observed that the future output data matrix, Y_f, is composed of the two major matrices (i.e., $\Gamma_i \cdot X_f$ and $H_i \cdot U_f$) that might not be orthogonal to each other, and also contains two noise matrices (i.e., $G_i \cdot W_f$ and V_f). Therefore, oblique projection can be used to derive the extended observability matrix. For noise contaminated cases in real applications, it was proved by Verhaegen (1994) that the original oblique projection matrix projects onto $U_{f(k)}^{\perp}$ orthogonally for noise conditions will derive satisfied results on estimating Γ_i. This is called "MOESP algorithm" (Multi-variable Output Error State sPace algorithm). The extended observability matrix Γ_i can be

achieved by conducting Singular Value Decomposition (SVD) on the oblique projection matrix $O_{(k)}^{Oblique}$.

Besides, the target projection matrix can also be directly computed from LQ decomposition on a certain arrangement of Hankel matrix that organizes "future input $U_{f(k)}$/ past instrumental variable $\Xi_{p(k)}$/ future output $Y_{f(k)}$ " in sequence, as shown below

$$
\begin{bmatrix} U_{f(k)} \\ \Xi_{p(k)} \\ Y_{f(k)} \end{bmatrix}_{2i(m+l) \times j} = \begin{bmatrix} L_{11(k)} & 0 & 0 \\ L_{21(k)} & L_{22(k)} & 0 \\ L_{31(k)} & L_{32(k)} & L_{33(k)} \end{bmatrix}_{2i(m+l) \times 2i(m+l)} \cdot \begin{bmatrix} Q_{1(k)}^T \\ Q_{2(k)}^T \\ Q_{3(k)}^T \end{bmatrix}_{2i(m+l) \times j} \tag{3}
$$

$$
O_{(k)}^{Oblique} = Y_{f(k)} /_{U_{f(k)}} \Xi_{p(k)} / U_{f(k)}^{\perp} = L_{32(k)} Q_{2(k)}^T
$$

then the product of LQ-elements $L_{32(k)} Q_{2(k)}^T$ is equal to the resultant projection matrix, without the need of explicitly executing the numerical operation of projection (Verhaegen and Dewilde 1992, Verhaegen 1993).

In summary, there are three basic steps on conducting offline subspace identification to extract the dynamic properties of a system. First, the measurements are collected to form the input as well as output data Hankel matrices; in this way, the state space model can be transformed into the matrix input-output equations. Second, either through orthogonal projection or oblique projection, the projection matrix $O_{(k)}^{Oblique}$ can be derived, in this step, a geometric projection can be conducted by either explicit expanding or through LQ decomposition. Finally, the SVD on the projection matrix $O_{(k)}^{Oblique}$ is used to extract the extended observability matrix Γ_i.

$$
O_{(k)}^{Oblique} = USV = \begin{bmatrix} U_1 & U_2 \end{bmatrix} \begin{bmatrix} S_1 & 0 \\ 0 & S_2 \end{bmatrix} \begin{bmatrix} V_1^T \\ V_2^T \end{bmatrix} \approx U_1 S_1 V_1^T \tag{4}
$$

$$
\Gamma_1 = U_1
$$

After the matrix Γ_i is calculated, the system matrices A_d and C_d can then be determined, and modal parameters can be further identified. For example, A_d can be obtained by least square approach.

$$
A_d = \underline{\Gamma_i}^{\dagger} \overline{\Gamma_i} = \begin{bmatrix} C_c \\ C_c A_d \\ C_c A_d^2 \\ \vdots \\ C_c A_d^{i-2} \end{bmatrix}^{\dagger} \cdot \begin{bmatrix} C_c A_d \\ C_c A_d^2 \\ C_c A_d^3 \\ \vdots \\ C_c A_d^{i-1} \end{bmatrix} \tag{5}
$$

Then, the natural frequency and the damping ratio can be derived from the eigenvalue decomposition of A_c.

$$
A_c = \log(A_d) \cdot SR \tag{6}
$$

where **SR** is the sampling rate.

To apply subspace identification, several user-defined parameters need to be properly assigned. The following user-defined parameters are described:

• Low-pass filter and down-sampling rate on the original data

Depends on the quality of the recorded signal, low-pass filter can be applied to extract the lower modes of the structural system. As for down-sampling rate, it is not recommended to use unless a lot of channel data needs to be implemented in subspace identification (to reduce the size of the data). The Butterworth low-pass filter as well as filtering signal using wavelet packet transform (WPT) are recommended.

• Determine number of block row (i) in data Hankel matrix

The flock row in data Hankel matrix needs to cover the length of the fundamental period of the structure. It can be decided using the following formula

$$i = SR/(2 \times f_1) = 50/(2 \times 1) = 25$$

where f_1 is the fundamental frequency of the structure.

• Identify the structural modes using stabilization diagram to remove the spurious modes (it will be discussed in section 2.2).

2.2 Stabilization diagrams to distinguish physical modes and spurious modes

To identify the structural modes, the stabilization diagram is used. The stabilization diagram is simply a plot of different model orders versus the damping ratios or the frequencies identified at each of the model orders. The aim is that physical modes should show up with consistent frequencies, damping ratios, and mode shapes at various model orders whereas the spurious ones could be expected to show more erratic behavior. To remove the spurious modes, the following criteria are used:

(a) Check the stability of the identified modal parameters (i.e., natural frequency, damping ratio, and mode shape) from two different modal order. The conventional criteria based on modal parameters are shown as follows

$$\left|\frac{f_j - f_i}{f_i}\right| \leq \varepsilon_f \quad , \quad \left|\frac{\xi_j - \xi_i}{\xi_i}\right| \leq \varepsilon_\xi \quad \text{and} \quad MAC(\Phi *_j \cdot \Phi_i) = \frac{\left|\Phi *_j \cdot \Phi_i\right|^2}{(\Phi *_j \cdot \Phi_j)(\Phi *_i \cdot \Phi_i)} \geq MAC_\phi \tag{7}$$

(b) Check the model phase collinearity (MPC). The MPC indicates whether the mode shape components of a single mode lie on a straight line in the complex plane or not. For a particular mode, all locations on the structure should vibrate exactly in-phase or out-of-phase with one another. The MPC quantifies the degree of mode shape behavior by comparing the relative size of the eigenvalues of the variance-covariance matrix

3. Results of identification

Two seismic event data (San Fernando earthquake, 2001, and Newhall earthquake, 2011) recorded from the Pacoima dam are used to identify the dynamic characteristics of the dam during earthquake excitation. Totally, there are 17 channels of acceleration measurements in both seismic events. The recorded data along the abutment, from Channel 9 to Channel 17, are considered as

(a) San Fernando earthquake (1/13/2001)   (b) Newhall earthquake (9/1/2011)
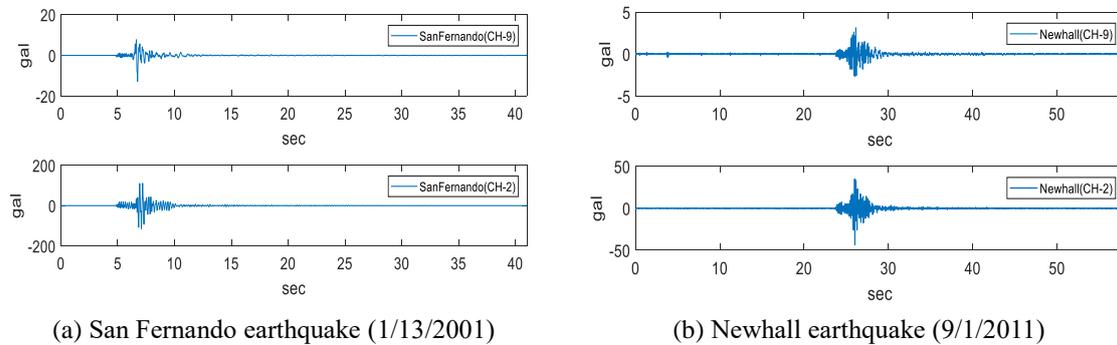
Fig. 2 Recorded acceleration at Channel 2 and Channel 9 of Pacoima dam

(a) San Fernando earthquake   (b) Newhall earthquake
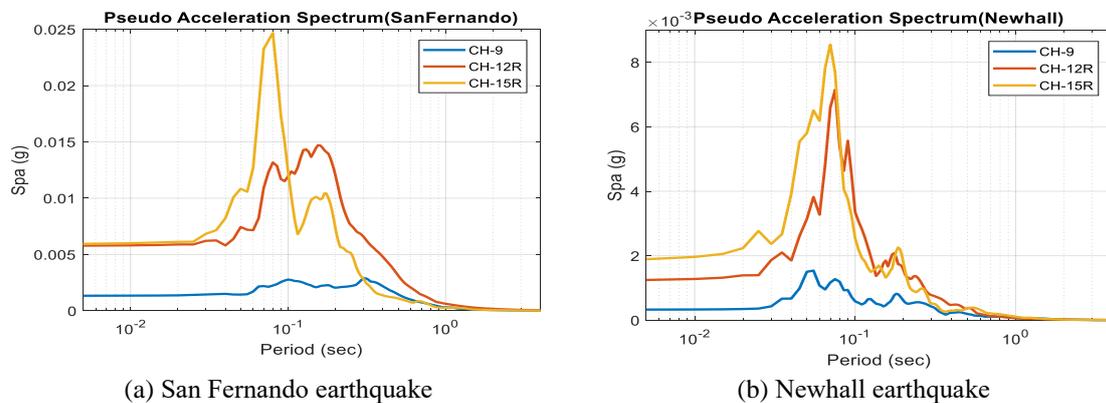
Fig. 3 Acceleration response spectrum of two set of seismic data from the dam abutment

inputs and the others, from Channel 1 to Channel 8, are considered as outputs. In particular, Fig. 2 shows the recorded acceleration from the dam abutment (the bottom abutment, Channel 2) and the dam crest (the middle crest, Channel 9) for both seismic events. The recorded peak acceleration at the dam crest in the radial direction for San Fernando earthquake is 0.164 g and depth 8.8 km, and for Newhall earthquake is 0.045 g and depth 0.1 km. The acceleration response spectrum from three input records along the dam abutment (Channel 9, 12 and 15) is also shown in Fig. 3. From the shape of response spectrum, it is interesting to see the spatially nonuniform distribution of motion along the canyon-shape abutment of the dam. The difference in the acceleration response spectrum from the recorded data along the left bank abutment, right bank abutment and the bottom of the dam is obvious.

3.1 Determine the data length for subspace identification

Generally, for system identification, there is no need to use the entire recorded data, because the high noise to signal ratio (N/S) in the pre-event memory data as well as the low amplitude data before the main shock may content. To avoid the influence of ambient noise on the result of identification, one needs to determine the strong motion duration and only use the data from the

strong motion duration for system identification. In this study, the concept of Akaike information criteria (AIC) picker (Zhang *et al.* 2003) is used to detect the P-wave arrival. The function form of AIC(k) at k-th time interval is shown in the following equation

$$AIC(k) = k * \log(\text{var } x[1,k]) + (N - k + 1) * \log(x[k+1, N]) \tag{8}$$

where N is the total number of data point and var x [1, k] is defined as the variance of signal x(t) from t=1 to t=k. In this study, the recorded acceleration data is used for x(t) to calculate the information criteria, AIC(k). As P-wave approaching, the AIC(k) will start to increase dramatically.

This instant of time can be automatically identified as the initial starting time of the record for analysis. There is no need to pre-assign any coefficient by using AIC(k) (different from using Arias Intensity) to determine the initial time. As for the end time of the record, one can select the time at 99.5 % of the Arias Intensity. As shown in Fig. 4, the strong motion duration is determined for both seismic event data for system identification.

3.2 Identification of model properties of Pacoima dam

Two seismic event data recorded from the seismic response of Pacoima dam are selected for this study: one is the San Fernando earthquake (2001) and the other is the Newhall earthquake (2011). Since the Pacoima dam has double curvature on the dam body, different from the system of building structure, the recorded data is transformed to the radial and tangential direction of the dam, as shown in Fig. 1(b) on Channel 12 and 14. The dynamic characteristics of the dam along the radial direction will be estimated. In order to capture the spatially nonuniform features of the seismic input along the dam abutment, three transformed data in the radial direction along the left, right, and bottom abutment are used as input and the data collected from the dam body in the radial direction are used as output. It is important to point out that using multiple inputs in subspace identification to consider the spatial variation of ground excitation along the dam abutment is necessary.

For cases of San Fernando earthquake and Newhall earthquake, before employing subspace identification, lowpass filter (Butterworth filter) with 50 Hz cut-off frequency was first applied. To remove the spurious modes from the stabilization diagram, the following two criteria are set: MAC=0.95 and MPC=0.90. Fig. 5 shows the stabilization diagram from the analysis of San Fernando earthquake. Fig. 5(a) is the case considering multiple input while Fig. 5(b) is the case considering single input from the bottom abutment (Channel 9). The size of data Hankel matrix is i=cl=160 for both cases. It is observed that three distinct model frequencies (i.e., ~3.7 Hz, ~4.5 Hz, and ~5.1 Hz) can be clearly identified from the stabilization diagram by using nonuniform input in subspace identification, while for case of single input only one stable mode can be identified. The mode shapes of the dam from the identified model frequencies are also shown in Fig. 6. Two identical mode shapes at frequency 3.7 Hz and 4.5 Hz (symmetric mode), respectively, are extracted from the San Fernando earthquake response data of the dam with the consideration of nonuniform input. Discussion of the identification of two identical mode shapes from San Fernando earthquake will be made in the following section.
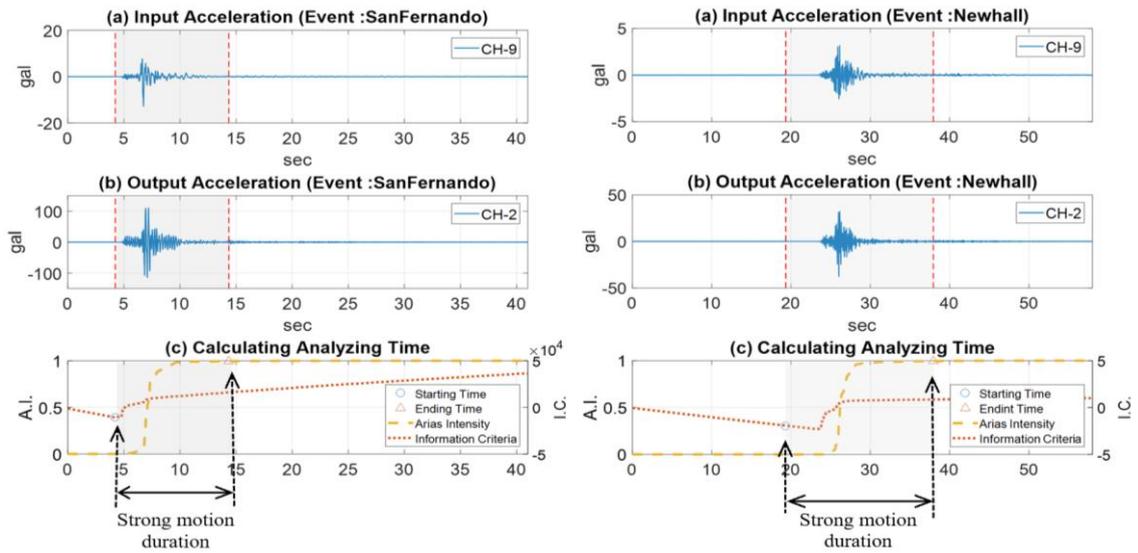
Fig. 4 Example to determine the strong motion duration for subspace identification; (a) & (b): Shaded area indicated the selected strong motion duration for analysis, (c) using IC index and 99.5% of Arias Intensity to determine strong motion duration
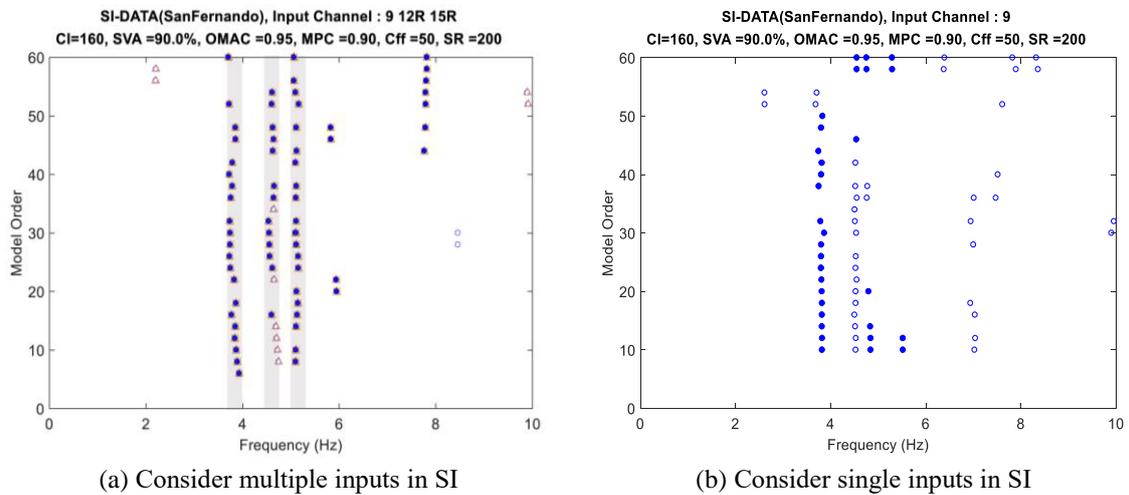
(a) Consider multiple inputs in SI   (b) Consider single inputs in SI

Fig. 5 Stabilization diagram from using San Fernando earthquake data (using cl=160)

The identification using Newhall earthquake data is also conducted. Fig. 7(a) shows the stabilization diagrams considering nonuniform input. A clear fundamental mode can be identified (i.e., 4.569 Hz). The identified mode shape is shown in Fig. 7(b). This identified mode shape is the same with 2nd mode shape identified from San Fernando earthquake. Different from the data collected from the San Fernando earthquake, obviously, only the fundamental mode of the dam can clearly be identified from the stabilization diagram. Since the Newhall earthquake event is a

small event (maximum peak acceleration of the dam response is 4.5 gal), the effect of dam-reservoir interaction is less significant as compared to the excitation of San Fernando earthquake.

In order to explain the two distinct frequencies with the same mode shape identified from the response data of San Fernando earthquake, two different approached will be discussed: (1) Time-frequency analysis on the response data, (b) Tune effect of dam-water interaction.

PacoimaDam(SanFernando), Input Channel : 9 12R 15R
Frequency = 3.7703 Hz, Damping = 1.4142%, Order =16
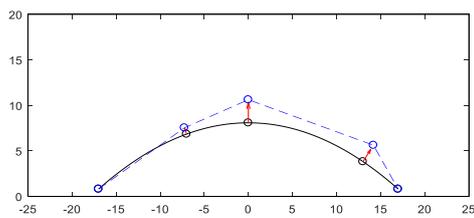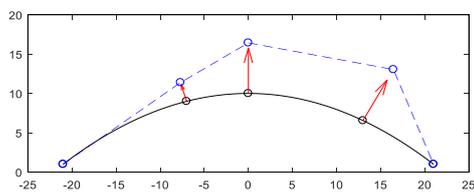
PacoimaDam(SanFernando), Input Channel : 9 12R 15R
Frequency = 4.5988 Hz, Damping = 1.8897%, Order =16
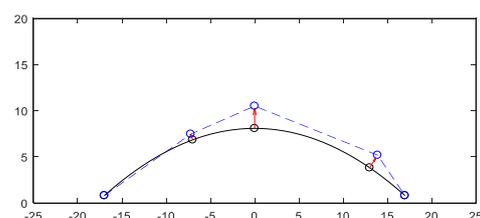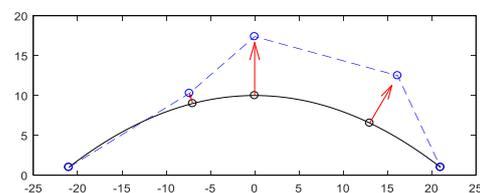
(a) Mode 1: f_1=3.7703 Hz and ξ_1=1.414%   (b) Mode 2: : f_2=4.599 Hz and ξ_2=1.889%

PacoimaDam(SanFernando), Input Channel : 9 12R 15R
Frequency = 5.1293 Hz, Damping = 10.1649%, Order =16
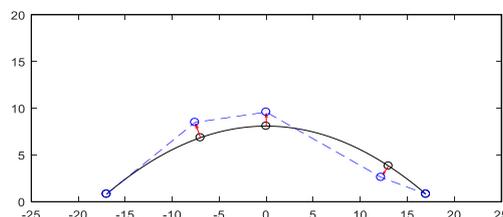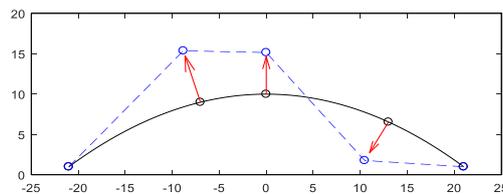
(c) Mode 3: : f_3=5.129 Hz and ξ_3=10.165%

Fig .6 Identified three modes of the Pacoima dam (at level 661 m and 637 m) using nonuniform input SI

SI-DATA(Newhall), Input Channel : 9 12R 15R
CI=140, SVA =95.0%, OMAC =0.95, MPC =0.90, Cff =50, SR =200

(a)

PacoimaDam(Newhall), Input Channel : 9 12R 15R
Frequency = 4.5698 Hz, Damping = 2.9327%, Order =20


(b)
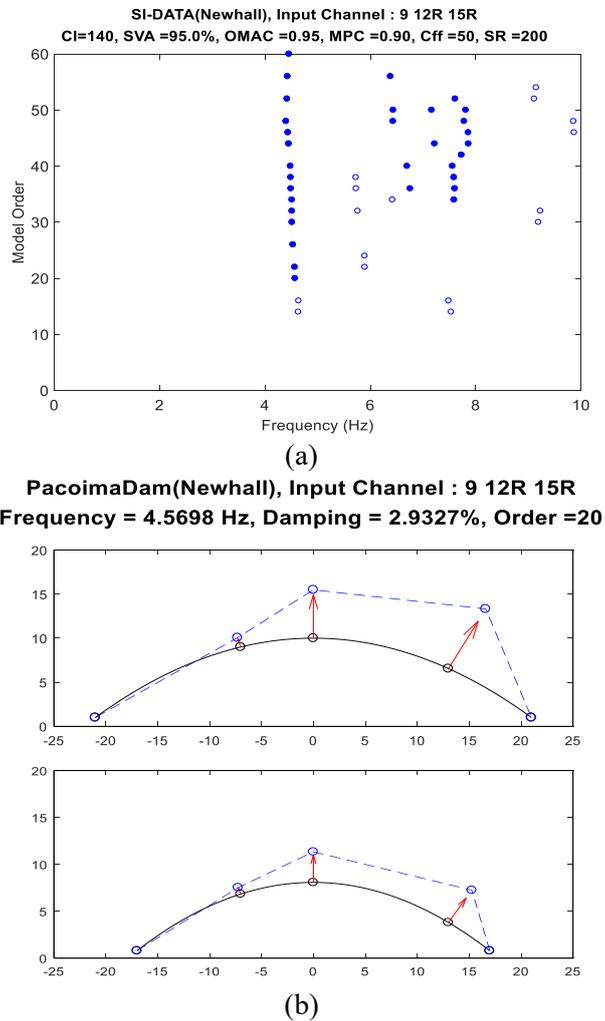
Fig. 7(a) Stability diagram from using Newhall earthquake data (using cl=140) and (b) Identified mode of the Pacoima dam from Newhall earthquake data (at level 661 m and 637 m)

3.3 Time-frequency analysis on seismic response measurement

To have a better visualization on the seismic response measurement of the dam, the wavelet analysis technique is used to decompose the measurement data from different seismic events. First, the modified complex Morlet wavelet (MCMW) is selected as the mother wavelet. The MCMW is essentially a complex exponential modulated by a Gaussian envelope, with σ as a measure for the time spread. The scaled wavelet is given by (Todorovska 2001)

$$\psi_{(b,a)}^{*}(t) = \frac{1}{\sqrt{a}} e^{i\omega_0(\frac{t-b}{a})} e^{-(\frac{t-b}{a})^2/2\sigma^2} \tag{9}$$

For the Morlet wavelet, there is a unique relationship between the scale parameter a and Fourier frequency ω. The scale parameter a is inversely proportional to frequency, i.e., $= \omega_0/\omega$. For the scale parameter $a < 1$ ($\omega_0 < \omega$), an increase in time resolution will result in a decrease in frequency resolution, and vice versa. As for the σ value, time duration increases for larger σ and the frequency bandwidth becomes narrower, which provides a smoother wavelet spectrum in the time axis and a sharper spectrum in the frequency axis, and vice versa. For using the modified Morlet wavelet analysis different σ value will be selected, so as to enhance the frequency as time resolution expands. In this study, instead of choosing different scales, different central frequencies (f_c) were chosen to fix the scale ($a = 1$) when the frequency changed, and consequently the coefficient $W_\psi[x](b,a)$ is changed to $W_\psi[x](b,\omega)$.

Seismic response data (from San Fernando earthquake, Newhall earthquake, and Chino Hills earthquake) collected from the dam crest in radial direction (Channel 2) is used for analysis (except Chino Hills earthquake). Among these three seismic event data, the San Fernando earthquake caused the peak acceleration of dam crest with peak acceleration of 0.164 g, and the other two events are with peak acceleration less than 0.05 g. Fig. 8 shows the wavelet coefficient (defined as spectrogram) of the three seismic event data collected from the center location of the dam crest (Channel 2 in radial direction). From the event of San Fernando earthquake, significant wavelet coefficients were observed between 3.5 Hz and 4.4 Hz, and around 4.8 Hz (as shown in Fig. 8(c)). It is observed that during the strong motion more complicated modes will be excited in between 3.5 Hz and 4.4 Hz (will be explained in the following section). As for the two small earthquake events (Newhall earthquake, and Chino Hills earthquake), from Figs. 8(a) and 8(b), it is observed that only a clear dominant wavelet coefficient with frequency around 4.4 Hz can be identified. Large wavelet coefficient at frequency around 5.7 Hz in the spectrogram of small earthquake event which can be explained as the excitation signal (will be explained later). To confirm the impact of the significant earthquake excitation on the response of the dam, two-time windows are chosen (1.0 ~15.0 sec and 15.0 ~ 40.0 sec) on the San Fernando earthquake to generate the spectrogram separately. Compare the spectrogram generated from two different time windows, as shown in Fig. 9, one can be observed that more complicate modes need to be investigated from the response of strong motion duration of San Fernando earthquake. The spectrogram of the base excitation data along the boundary of the dam was also generated, as shown in Fig. 10. It is observed that at Channel-9 (bottom of the dam) in radial direction, the dominant amplitude around frequency near 3.5 Hz is significant which can be explained as the dominant frequency of the input excitation (it is consistent with the dominant peak in the response spectrum of data from Channe-9).

3.4 Discussion on the dam-reservoir interaction during strong earthquake excitation

The application of subspace identification technique to the San Fernando earthquake response data of Pacoima dam, the identified mode shapes (symmetric mode) from the first two model frequencies in the stabilization diagram shows two similar mode shapes. This phenomenon is different from the identification of seismic response of building structure. Considering the dam-reservoir interaction during earthquake excitation, the excitation on the dam body is not only coming from the foundation motion of the dam but also has one additional effect (force) resulting from the fluid acting on the structure. This additional force is due to the unsteady motion of dam body underwater during ground motion. The phenomenon is attributed to the added mass of the

water. When a dam-reservoir system is subjected to a severe earthquake ground excitation, the hydrodynamic pressures are set up due to the vibration of the dam and reservoir and the dynamic behavior should be considered as a coupled dynamic interaction system. Generally, the added mass

(a) CH-2 of Newhall earthquake (σ=10)   (b) CH-5 of Chino Hills earthquake (σ=10)

(c) CH-2 of San Fernando earthquake (σ=4)
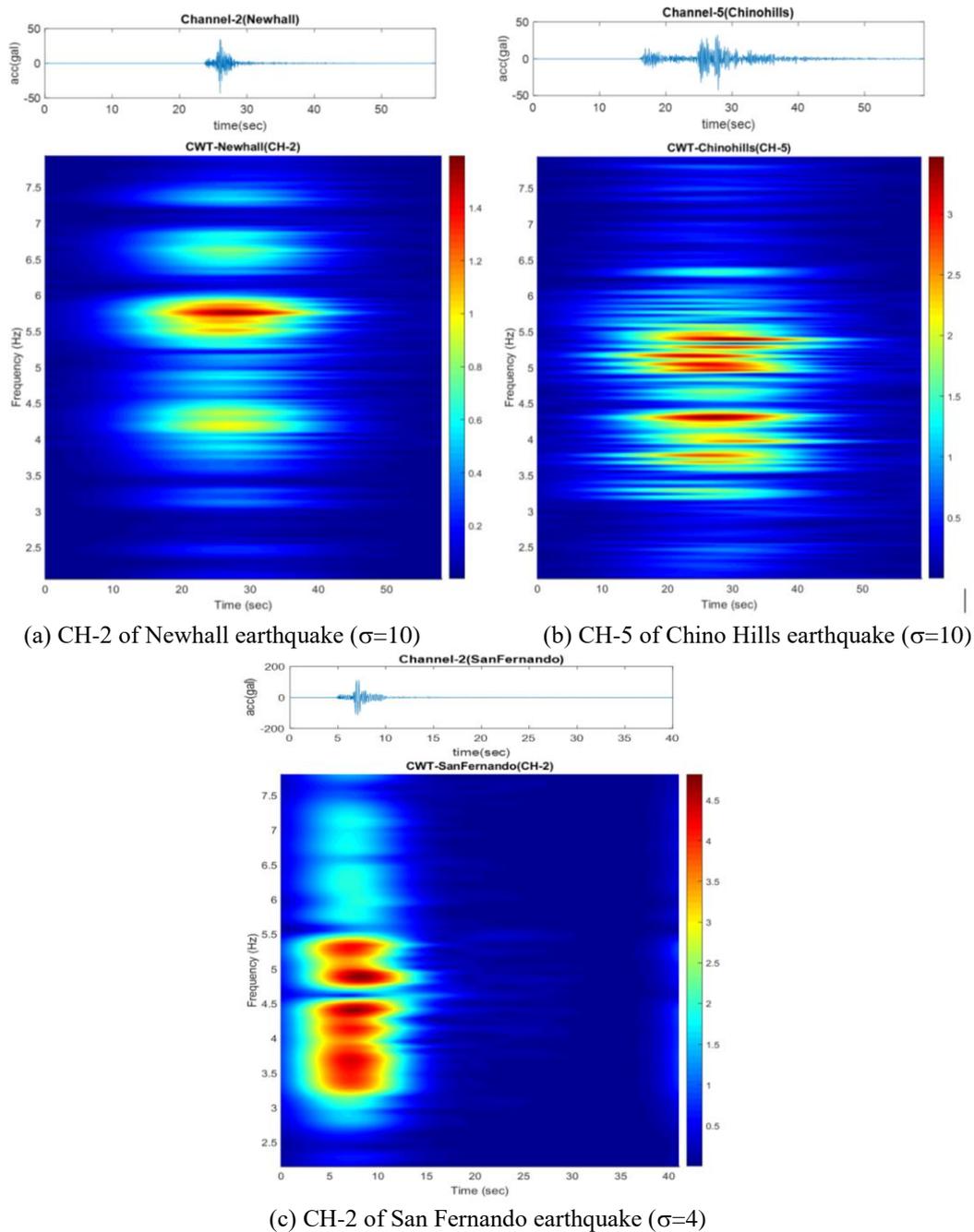
Fig. 8 Spectrogram of three seismic event data recorded from Pacoima dam

(a) Plot data from time window 0.0 ~ 15.0 sec　　　(b) Plot data from time window 15.0 ~ 40.0 sec
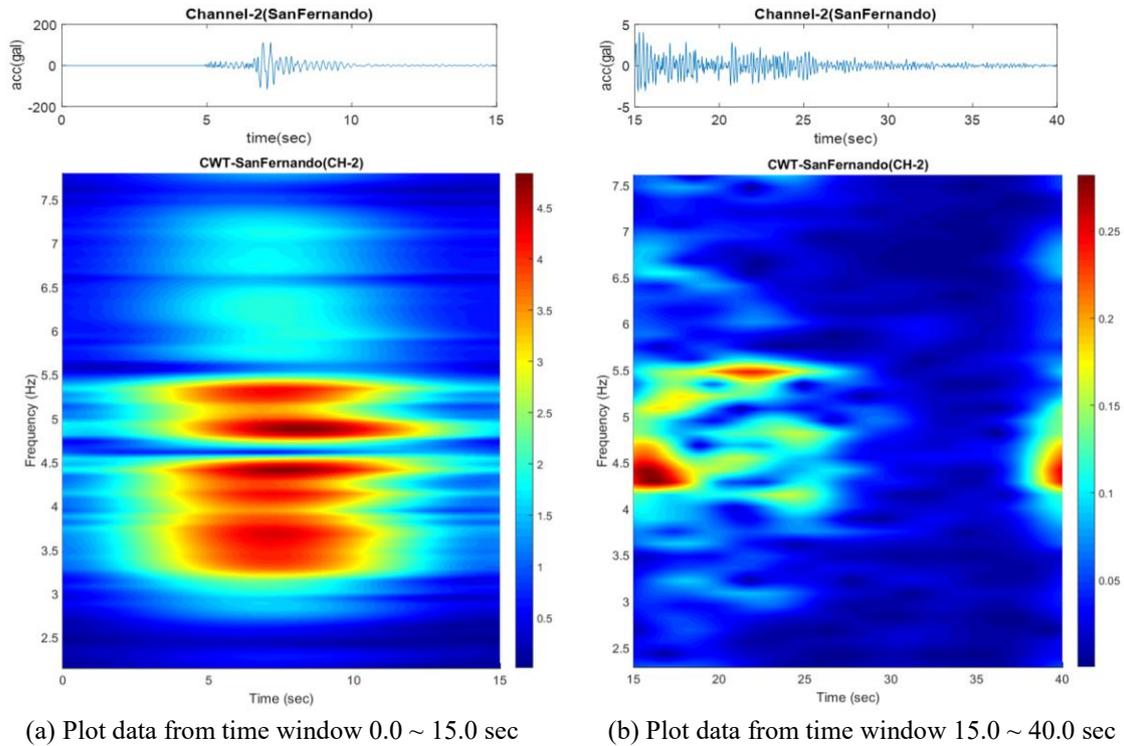
Fig. 9 Spectrogram of Chanel 2 data of Pacoima dam recorded from San Fernando earthquake

(a) Chanel-12　　　　　　　(b) Chanel-9　　　　　　　(c) Chanel-15
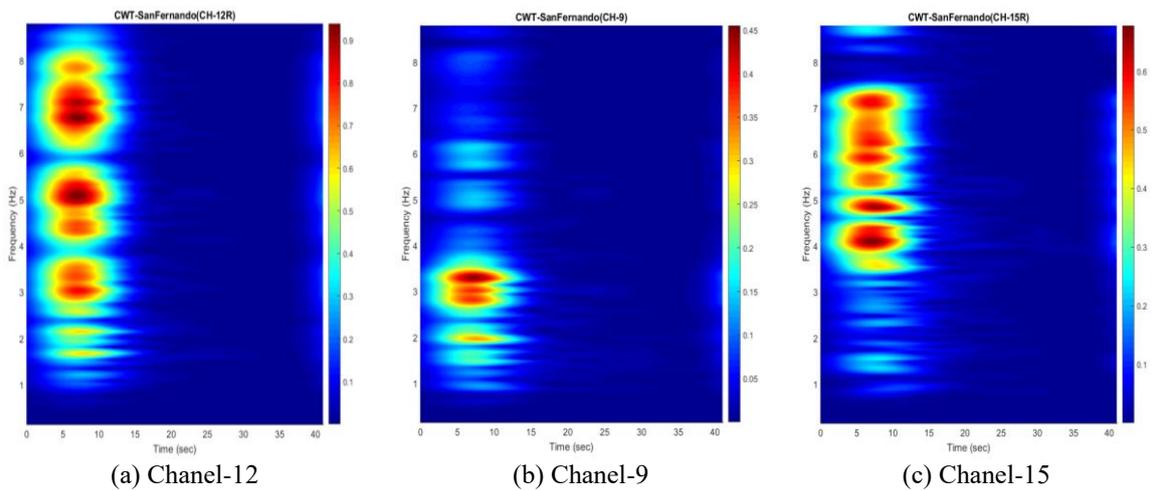
Fig. 10 Spectrogram of data recorded from San Fernando earthquake at Ch-12, Ch-9 and Ch-15 in radial direction along the foundation of the dam

of water to the structural system not only can reduce the dominant frequency of the structural system but also can induce a very complicated interaction between the dam body and the water. This phenomenon is even more obvious during strong ground motion than weak ground motion.

From the system identification of the dam data from San Fernando earthquake, one can identify two similar mode shapes in two different discrete frequencies. It is believed that, due to the added mass of water, the dam-reservoir interaction becomes significant which may create the tuned effect on the dam. To observe the two similar mode shapes, appear in two different dominant frequencies of the dam structure during earthquake excitation, a 2-degree-of-freedom system with a tuned mass damper at the top, as shown in Fig. 11, is simulated. This 2-DOF system with tuned mass damper (TMD) is subjected to base excitation with the same input of Channel 9 from San Fernando earthquake. In the simulation study, the original 2-DOF system has two fundamental model frequencies as 1.341 Hz and 2.637 Hz, respectively. This 2-DOF system is implemented with a TMD, and the parameters of the TMD is assumed to have a damping ratio of 11% and a natural frequency of 1.21 Hz (Sadek *et al*. 1997). The designed parameter of the system is shown in Table 1. The structure is subjected to one-dimensional base excitation (using the recorded data from the bottom abutment during the San Fernando earthquake) and the acceleration response is simulated using the state space model in Chapter 2. To identify the structural system, only the data collected from the response of the lumped-mass structural system was used (without using the response data from TMD). The subspace identification technique was also employed to identify the dynamic characteristics of the TMD system. This approach is trying to simulate the dam-reservoir interaction and to explain the result from identification of dam under earthquake excitation. Similar to the study of dam-reservoir interaction, the water in the reservoir can be considered as an added mass on the dam body. For system identification the response of TMD cannot be measured in the simulation study; only the responses of primary structural system can be measured for system identification. Since the TMD system is coupled with the primary system, by using the structural response for identification, one can clearly identify three modes from the stabilization diagram. Because only two measurements are used, the two fundamental modes with the same mode shapes can be extracted. This indicated the effect of dam-reservoir interaction near the fundamental mode of the structural system. Fig. 12 shows the stabilization diagram as well as the identified mode shapes of the model. It is observed that two model frequencies f1=1.102 Hz and f2=1.474 Hz with the same mode shape are identified and the 3rd model frequency with different mode shapes is 2.641 Hz (same as the 2nd mode of the original structure).

System Natural Frequency	1.341 Hz (1st mode), 2.637 Hz (2nd Mode)
M_d/M_1 (mass ratio of TMD)	10 % of m1
TMD natural frequency	1.2141 Hz (ξ= 6.27%)

(a) 3-DOF system with TMD   (b) Design parameterts of the TMD system
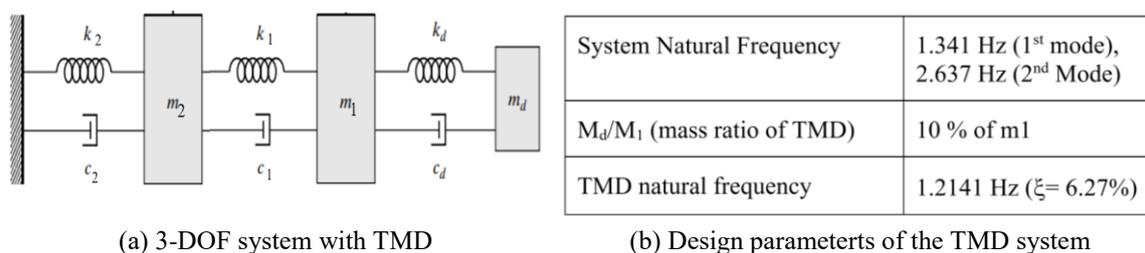
Fig. 11 Simulation of 2-DOF system with tuned mass

(a)

(b)
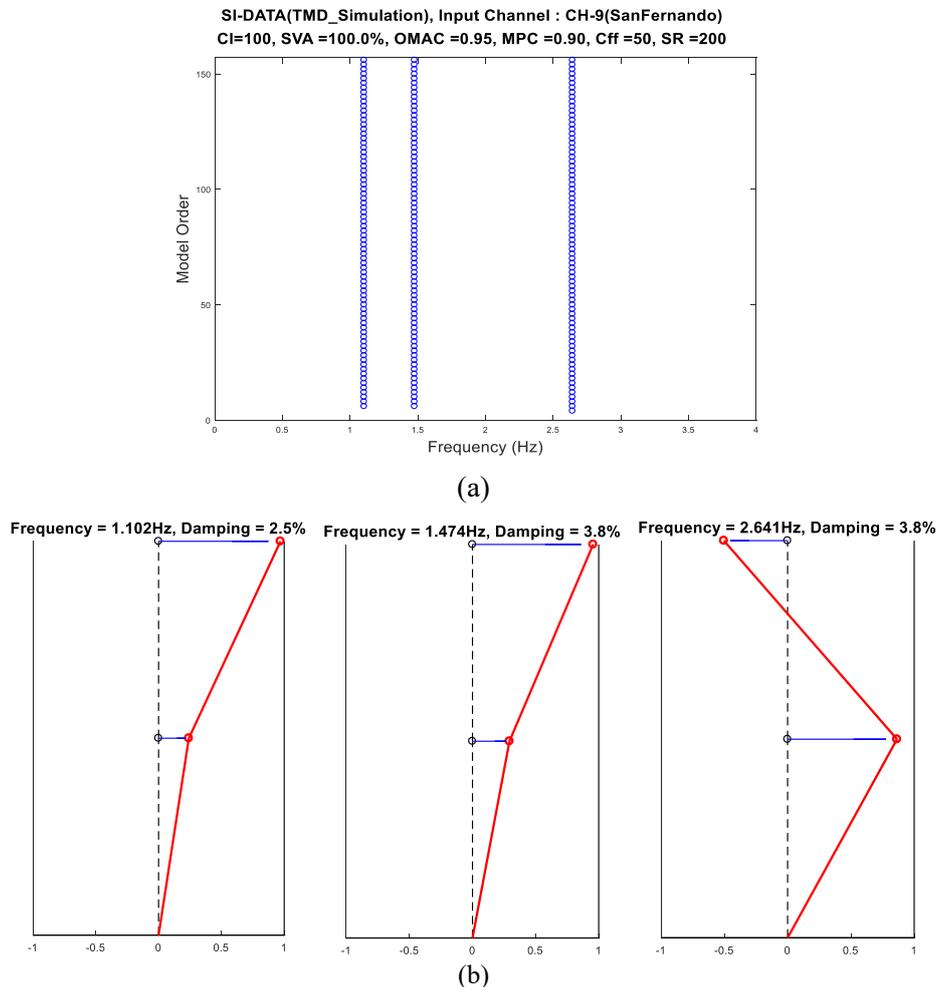
Fig. 12 (a) Stabilization diagram using response data from the 3-DOF system (with tuned mass) and (b) Identified mode shapes from the simulated TMD system.

The identified two mode shapes at two tuned model frequencies (f1=1.102 Hz and f2=1.474 Hz) have similar mode shapes which is simply due to the tuned effect of the added mass. This result is the same as the identification result of dam-reservoir interaction from the Pacoima dam during San Fernando earthquake. Through this simulation study, it is observed that during the strong ground motion (such as San Fernando earthquake), the effect of added mass on dam-reservoir interaction is significant, and the added mass from water may create the tuned effect on the dam body and develop two separate frequencies with similar mode shapes. On the contrary, for small earthquake event data (such as the data from Newhall earthquake), the effect of added mass from the reservoir is insignificant. Therefore, there is almost no dam-reservoir interaction and the tuned mass effect from the water for small event of earthquake excitation.

4. Conclusions

Two seismic response data collected from the strong motion instrumentation of Pacoima dam are analyzed.   The subspace identification (SI) technique is used to identify the model frequencies and mode shapes of the dam structure in the radial direction during earthquake excitation. Different from the identification of the seismic response of building structure using parametric model, the state-space equation is used together with the measurement data along the dam abutment as input to consider the nonuniform input ground motion. It is a multivariate signal processing method. The advantages of using subspace identification are:
• A good initial model can be quickly obtained with subspace methods.
• Simple parametrization for MIMO systems and robust noniterative numerical solutions.
• Reliable numerical tools-based LQ decomposition and singular value decomposition (SVD) are used to extract system dynamic characteristics.
From the recorded data of San Fernando earthquake from Pacoima dam, two identical modes corresponding to two different model frequencies are identified. This phenomenon can be explained as the tuned effect of dam-reservoir interaction. Through the simulation of 2-DOF system with TMD, with the suitable design parameters of the TMD, one can also identify the same result. This simulation proofs the significant dam-reservoir interaction of Pacoima dam under San Fernando earthquake. On the contrary, for a small seismic event (such as Newhall earthquake), the dam-reservoir interaction is insignificant, therefore, one can only identify the fundamental frequency of the system and the tuned effect cannot be observed.

Acknowledgments

References

Favoreel, W., De Moor, B. and Van Overschee, P. (2000), "Subspace state space system identification for industrial processes", *J. Process Control*, **10**(2-3), 149-155. https://doi.org/10.1016/S0959-1524(99)00030-X.
Fujita, K., Ikeda, A., Shirono, M. and Takewaki, I. (2015), "System identification of high-rise buildings using shear-bending model and ARX model: Experimental investigation", *Earthq. Struct.*, **8**(4), 843-857. https://doi.org/10.12989/eas.2015.8.4.843.
Junag, J.N. (1994), *Applied System Identification*, Prentice Hall PTR, Upper Saddle River, NJ, USA.
Kameyama, K., *et al.* (2005), "Recursive 4SID-based identification algorithm with fixed input-output data size", *Int. J. Innov. Comput. Inform. Control*, **1**(1), 17-33. https://www.researchgate.net/publication/228745503.
Larimore, W.E. (1994), "The optimality of canonical variate identification by example", *Proceedings of the SYSID'94*, Copenhagen, Denmark. https://doi.org/10.1016/S1474-6670(17)58319-6.
Li, H.N., Yi, T.H., Ren, L., Li, D.S. and Huo, L.S. (2014), "Reviews on innovations and applications in structural health monitoring for infrastructures", *Struct. Monit. Maint.*, **1**(1), 001-045. http://dx.doi.org/10.12989/smm.2014.1.1.001.

Ljung, L. (1999), System Identification Theory for User, Second edition, Prentice Hall, Upper Saddle River, NJ, USA.

Loh, C.H. and Wu, T.S. (2000), "System ID of Fei-Tsui Arch Dam from Forced Vibration and Seismic Response Data" , *J. Earthq. Eng.*, **4**(4), 511-537. https://doi.org/10.1080/13632460009350381.

Oku, H. (2007), "Recursive subspace model identification algorithms for slowly time-varying systems in closed loop", European Control Conference (ECC), July, Greece. https://doi.org/10.23919/ECC.2007.7068366.

Rao, B.D. and Arun, K.S. (1992), "Model based processing of signals: a state space approach", *Proceedings of IEEE*, **80**(2), 283-309. https://ieeexplore.ieee.org/document/123298.

Sadek, F., Mohraz, B., Taylor, A.W. and Chung, R.M. (1997), "A method of estimating the parameters of tuned mass dampers for seismic applications", *Earthq. Eng. Struct. D.*, **26**(6), 617-635. https://doi.org/10.1002/(SICI)1096-9845(199706)26:6<617::AID-EQE664>3.0.CO;2-Z.

Söderström, T. and Stoica, P. (1989), *System Identification*, Prentice Hall International, USA.

Todorovska, M.I. (2001), *Estimation of instantaneous frequency of signals using the continuous wavelet transform*, Dept. of Civil Engrg., Univ. of Southern California, Report CE 01-07, CA, USA.

Van Der Veen, A.J., Deprettere, E.D.F. and Swindlehurst, A.L. (1993), "Subspace-based signal analysis using singular value decomposition", *Proceedings of IEEE*, **81**(9), 1277-1308. https://ieeexplore.ieee.org/document/237536.

Van Overschee, P. and De Moor, B.L. (1994), "N4SID: subspace algorithms for the identification of combined deterministic stochastic systems", *Automatica*, **30**(1), 75-93. https://www.sciencedirect.com/science/article/pii/0005109894902305

Van Overschee, P. and De Moor, B.L. (1996), *Subspace identification for linear systems: theory-implementation-applications*, Boston/London/Dordrecht: Kluwer Academic Publishers.

Verhaegen, M. (1993), "Subspace model identification Part 3. Analysis of the ordinary output-error state-space model identification algorithm". *Int. J. Control*, **58**(3), 555-586. https://doi.org/10.1080/00207179308923017.

Verhaegen, M. (1994), "Identification of the deterministic part of MIMO state space models given in innovations from input-output data", *Automatica*, **30**(1), 61-74. https://www.sciencedirect.com/science/article/pii/0005109894902291.

Verhaegen, M. and Dewilde, P. (1992), "Subspace model identification part 2. Analysis of the elementary output-error state-space model identification algorithm", *Int. J. Control*, **56**(5), 1211-1241. https://doi.org/10.1080/00207179208934364.

Viberg, M. (1994), "Subspace methods in system identification", *Proceedings of the SYSID '94*, Copenhagen, Denmark. https://www.sciencedirect.com/science/article/pii/S1474667017476890.

Zhang, H.J., Thurber, C. and Rowe, C. (2003), "Automatic P-Wave Arrival Detection and Picking with Multiscale Wavelet Analysis for Single-Component Recordings", *Bull. Seismol. Soc. Am.*, **93**(5), 1904-1912. https://doi.org/10.1785/0120020241.

JK